

# Applications of regularized meshless method in engineering problems

Jeng-Hong Kao<sup>1\*</sup>, Kue-Hong Chen<sup>2</sup>, Jeng-Tzong Chen<sup>1</sup>

<sup>1</sup> Department of Harbor and River Engineering, National Taiwan Ocean University

<sup>2</sup> Department of Information Management, Toko University

\*Jenghung.kao@gmail.com

**NSC PROJECT: NSC 95-2221-E-464-003-MY3**

## ABSTRACT

In this paper, we employ the regularized meshless method (RMM) to solve antiplane shear and antiplane piezoelectricity problems with a multiple inclusions and acoustic eigenproblem with multiply-connected domain. The solution is represented by a distribution of double-layer potentials. The subtracting and adding-back technique is used to regularize the singularity and hypersingularity of the kernel functions. Only boundary nodes on the real boundary are required by using the proposed technique in a different way of conventional MFS by distributing singularities on fabricated boundary. Finally, the numerical results demonstrate the accuracy of the solutions after comparing with analytical solutions and those of BEM, FEM and PM. Good agreements are obtained.

**Keywords:** regularized meshless method, subtracting and adding-back technique, method of fundamental solutions, piezoelectricity, multiple inclusions, multiple holes, spurious eigenvalue, acoustics.

## 1. INTRODUCTION

Bleustein (1968) [1] investigated the antiplane piezoelectric dynamics problem and discovered the existence of Bleustein wave. Pak (1992) [2] has considered a more general case by introducing a piezoelectric inclusion which, in the limiting case of vanishing elastic and piezoelectric constants, become a permeable hole containing free space with electric fields. He obtained an analytical solution by using the alternative method. Later, Honein *et al.* (1995) [3] have visited the problem of two circular piezoelectric fibers subjected to out-of-plane displacement and in-plane electric field. In 1997, Chen and Chiang [4] solved for 2D problems of an infinite piezoelectric medium containing a solitary cavity or rigid inclusion of arbitrary shape, subjected to a coupled anti-plane mechanical and in-plane electric load at the matrix by using the conformal mapping techniques. In recent years, Chao and Chang [5] studied the stress concentration and tangential stress distribution on double piezoelectricity inclusions by using the complex variable theory and the method of successive approximations. The antiplane shear problem [6, 7] is a limiting case of antiplane piezoelectricity

problem, when electric fields and piezoelectric modulus approximate to zero.

For the acoustic eigenproblem with a multiply-connected domain, spurious eigensolutions always appear, even when the complex-valued BEM is employed to solve the eigensolutions [8]. In Chen *et al.* work of [8], the problem of spurious eigensolutions of the singular and hypersingular BEMs was studied by using circulant for an annular case and treated by using the Burton & Miller approach in a discrete system. Chen *et al.* [9] studied spurious and true eigensolutions for a multiply-connected problem by using BIE, BEM and dual BEM. Also, spurious eigensolutions were examined in the MFS for annular eigenproblems [10]. In this study, we propose a meshless method to solve engineering problems.

To simplify complexity of numerical methods in the preprocessor of data preparation, meshless methods were developed to accelerate the speed of model creation. The mesh reduction techniques possess a great promise to replace the FEM and BEM as a dominant numerical method. Because of neither domain nor surface meshing are required for the meshless method, it is very attractive for engineering communities. In this study, we solve antiplane shear and antiplane piezoelectricity problems with multiple inclusions and acoustic eigenproblem with a multiply-connected domain by using proposed meshless method. Spurious eigenvalues are extracted out by employing SVD updating term technique. The method of fundamental solutions (MFS) is one of the meshless methods and belongs to a boundary method for boundary value problems, which may be viewed as a discrete type of indirect boundary element method. In the MFS [11], the solution is approximated by a set of fundamental solutions which are expressed in terms of sources located outside the physical domain. The unknown coefficients in the linear combination of the fundamental solutions are determined by matching the boundary condition. The method is relatively easy to implement. It is adaptive in the sense that it can take into account sharp changes in the solution and in the geometry of the domain and can easily treat with complex boundary conditions. A survey of the MFS and related method over the last thirty years has been found [11]. However, the MFS is still not a popular method because of the debatable artificial boundary distance of source location in numerical

implementation especially for a complicated geometry. The diagonal coefficients of influence matrices are divergent in the conventional case when the fictitious boundary approaches the physical boundary. In spite of its gain of singularity free, the influence matrices become ill-posed when the fictitious boundary is far away from the physical boundary. It results in an ill-posed problem since the condition number for the influence matrix becomes very large.

Recently, we developed a modified MFS, namely regularized meshless method (RMM), to overcome the drawback of MFS for solving the Laplace and Helmholtz problems [12, 13, 14]. The method eliminates the well-known drawback of equivocal artificial boundary. The subtracting and adding-back technique [12, 13, 14] is implemented to regularize the singularity and hypersingularity of the kernel functions. This method can simultaneously distribute the observation and source points on the physical boundary even using the singular kernels instead of non-singular kernels. The diagonal terms of the influence matrices can be extracted out by using the proposed technique.

In this study, the RMM is extended to solve three engineering problems. The results are compared with analytical solutions [3, 6, 9] to show the validity of our method.

## 2. Formulation

### 2.1 Governing Equation and Boundary Conditions

#### (1) Acoustic eigenproblem with a multiply-connected domain

Consider an eigenproblem with an acoustic pressure field  $u(x)$ , which satisfies the Helmholtz equation as follows:

$$(\nabla^2 + k^2)u(x) = 0, \quad x \in D, \quad (1)$$

subject to boundary conditions,

$$u(x) = \bar{u} = 0, \quad x \in B_p^u, \quad p = 1, 2, 3, \dots, m \quad (2)$$

$$t(x) = \bar{t} = 0, \quad x \in B_q^t, \quad q = 1, 2, 3, \dots, m \quad (3)$$

where  $\nabla^2$  is the Laplacian operator,  $k$  is the wave number,  $D$  is the domain of the problem,  $t(x) = \partial u(x) / \partial n_x$ ,  $m$  is the total number of boundaries including  $m-1$  numbers of inner boundaries and one outer boundary (the  $m$ th boundary),  $B_p^u$  is the essential boundary (Dirichlet boundary) of the  $p$ th boundary in which the potential is prescribed by  $\bar{u}$  and  $B_q^t$  is the natural boundary (Neumann boundary) of the  $q$ th boundary in which the flux is prescribed by  $\bar{t}$ . Both  $B_p^u$  and  $B_q^t$  construct the whole boundary of the domain  $D$  as shown in Fig. 1(a).

#### (2) Antiplane shear and antiplane piezoelectricity problems with multiple inclusions

Consider piezoelectric inclusions embedded in an infinite domain as shown in Fig. 2(a). The inclusions and matrix have different material properties. The matrix is subjected to a remote antiplane shear,  $\sigma_{zy} = \tau$ , and a remote inplane electric field,  $E_y = E_\infty$ . A uniform

electric field can be induced in piezoelectric material by applying a potential field  $E = E_\infty$ .

For this problem, the out-of-plane elastic displacement  $w$  and the electric potential  $\phi$  are only functions of  $x$  and  $y$ , such that

$$w = w(x, y), \quad \phi = \phi(x, y). \quad (4)$$

The equilibrium equations for the stresses and the electric displacements are

$$\partial \sigma_{zx} / \partial x + \partial \sigma_{zy} / \partial y = 0, \quad \partial D_x / \partial x + \partial D_y / \partial y = 0, \quad (5)$$

where  $\sigma_{zx}$  and  $\sigma_{zy}$  are the shear stresses, while  $D_x$  and  $D_y$  are the electric displacements. For linear piezoelectric materials, the constitutive relations are written as

$$\begin{aligned} \sigma_{zx} &= c_{44}\gamma_{zx} - e_{15}E_x, & \sigma_{zy} &= c_{44}\gamma_{zy} - e_{15}E_y, \\ D_x &= e_{15}\gamma_{zx} + \epsilon_{11}E_x, & D_y &= e_{15}\gamma_{zy} + \epsilon_{11}E_y, \end{aligned} \quad (6)$$

in which  $\gamma_{zx}$  and  $\gamma_{zy}$  are the shear strains,  $E_x$  and  $E_y$  are the electric fields,  $c_{44}$  is the elastic modulus,  $e_{15}$  denotes the piezoelectric modulus and  $\epsilon_{11}$  represents the dielectric modulus. The shear strains  $\gamma_{zx}$  and  $\gamma_{zy}$  and the electric fields  $E_x$  and  $E_y$  are obtained by taking gradient of the displacement potential  $w$  and the electric potential  $\phi$  by the following relations:

$$\begin{aligned} \gamma_{zx} &= \partial w / \partial x, & \gamma_{zy} &= \partial w / \partial y, \\ E_x &= -\partial \phi / \partial x, & E_y &= -\partial \phi / \partial y. \end{aligned} \quad (7)$$

Substituting Eqs. (6) and (7) into (5), we obtain the following governing equations:

$$\begin{cases} c_{44}\nabla^2 w + e_{15}\nabla^2 \phi = 0 \\ e_{15}\nabla^2 w - \epsilon_{11}\nabla^2 \phi = 0 \end{cases} \quad (8)$$

From Eq. (8), we can obtain the equations as

$$\nabla^2 w = 0, \quad \nabla^2 \phi = 0, \quad (9)$$

where  $\nabla^2$  is the Laplacian operator. The continuity conditions across the matrix-inclusion interface are written as

$$w^i = w^m, \quad \sigma_{zx}^i = \sigma_{zx}^m, \quad (10)$$

$$\phi^i = \phi^m, \quad D_x^i = D_x^m, \quad (11)$$

where the superscripts  $i$  and  $m$  denote the inclusion and material, respectively. The loading is remote shear.

For the antiplane shear problem, we consider inclusions embedded in an infinite matrix as shown in Fig. 2(b). The inclusions and matrix have different elastic properties. When electric field and piezoelectric modulus approximate to zero, we can obtain governing equation and continuity conditions as

$$\partial^2 w / \partial x^2 + \partial^2 w / \partial y^2 = \nabla^2 w = 0, \quad (12)$$

$$w^i = w^m, \quad \sigma_{zx}^i = \sigma_{zx}^m. \quad (13)$$

### 2.2 Conventional Method of Fundamental Solutions

#### (1) Acoustic eigenproblem with a multiply-connected domain

By employing the RBF technique [10], the representation of the solution for a multiply-connected problem as shown in Fig. 1(a) can be approximated in terms of the  $\alpha_j$  strengths of the singularities at  $s_j$  as

$$\begin{aligned}
 u(x_i) &= \sum_{j=1}^N T(s_j, x_i) \alpha_j \\
 &= \sum_{j=1}^{N_1} T(s_j, x_i) \alpha_j + \sum_{j=N_1+1}^{N_1+N_2} T(s_j, x_i) \alpha_j + \cdots \\
 &\quad + \sum_{j=N_1+N_2+\cdots+N_{m-1}+1}^N T(s_j, x_i) \alpha_j,
 \end{aligned} \quad (14)$$

$$\begin{aligned}
 t(x_i) &= \sum_{j=1}^N M(s_j, x_i) \alpha_j \\
 &= \sum_{j=1}^{N_1} M(s_j, x_i) \alpha_j + \sum_{j=N_1+1}^{N_1+N_2} M(s_j, x_i) \alpha_j + \cdots \\
 &\quad + \sum_{j=N_1+N_2+\cdots+N_{m-1}+1}^N M(s_j, x_i) \alpha_j,
 \end{aligned} \quad (15)$$

where  $x_i$  and  $s_j$  represent the  $i$ th observation point and the  $j$ th source point, respectively,  $\alpha_j$  are the  $j$ th unknown coefficients (strength of the singularity),  $N_1, N_2, \dots, N_{m-1}$  are the numbers of source points on  $m-1$  numbers of inner boundaries, respectively,  $N_m$  is the number of source points on the outer boundary, while  $N$  is the total numbers of source points ( $N = N_1 + N_2 + \cdots + N_m$ ) and  $M(s_j, x_i) = \partial T(s_j, x_i) / \partial n_{x_i}$ . After matching boundary conditions, the coefficients  $\{\alpha_j\}_{j=1}^N$  are determined. The distributions of source points and observation points are shown in Fig. 1(a) for the MFS. The chosen bases are the double-layer potentials for the Helmholtz problem [14] as

$$T(s_j, x_i) = -(i\pi k / 2) H_1^{(1)}(kr_{ij}) ((x_i - s_j), n_j) / r_{ij}, \quad (16)$$

$$\begin{aligned}
 M(s_j, x_i) &= i\pi k / 2 \{ k H_2^{(1)}(kr_{ij}) \\
 &\quad ((x_i - s_j), n_j) ((x_i - s_j), \bar{n}_i) / r_{ij}^2 \\
 &\quad - H_1^{(1)}(kr_{ij}) n_k \bar{n}_k / r_{ij} \},
 \end{aligned} \quad (17)$$

where  $(\cdot, \cdot)$  is the inner product of two vectors,  $H_2^{(1)}(kr_{ij})$  is the second-order Hankel function of the first kind,  $r_{ij} = |s_j - x_i|$ ,  $n_j$  is the normal vector at  $s_j$ , and  $\bar{n}_i$  is the normal vector at  $x_i$ .

It is noted that the double-layer potentials have both singularity and hypersingularity when source and field points coincide, which leads to difficulty in the conventional MFS. The fictitious distance between the fictitious (auxiliary) boundary ( $B'$ ) and the physical boundary ( $B$ ), defined by  $d$ , shown in Fig. 1(a) needs to be chosen deliberately. To overcome the above mentioned shortcoming,  $s_j$  is distributed on the real boundary, as shown in Fig. 1(b), by using the proposed regularized technique as stated in the following Section 2.3. The rationale for choosing double-layer potential as the form of RBFs instead of the single-layer potential in the RMM is to take the advantage of the regularization of the subtracting and adding-back technique, so that no fictitious distance is needed when evaluating the diagonal coefficients of influence matrices which will be explained in Section 2.4. The single-layer potential can not be chosen because the following Eq. (23) in Section 2.3 is not provided. If the single layer potential is used, the regularization of subtracting and adding-back

technique can not work [12].

### 2.3 Regularized Meshless Method

(1) *Acoustic eigenproblem with a multiply-connected domain*

When the collocation point  $x_i$  approaches the source point  $s_j$ , the potentials in Eqs. (16) and (17) are approximated by:

$$\lim_{x_i \rightarrow s_j} T(s_j, x_i) = \bar{T}(s_j, x_i) = -n_k y_k / r_{ij}^2, \quad (18)$$

$$\begin{aligned}
 \lim_{x_i \rightarrow s_j} M(s_j, x_i) &= \bar{M}(s_j, x_i) + ik^2 / 4 \\
 &= (2((x_i - s_j), n_j) ((x_i - s_j), \bar{n}_i) / r_{ij}^4 \\
 &\quad - (n_j, \bar{n}_i) / r_{ij}^2) + ik^2 / 4,
 \end{aligned} \quad (19)$$

by using the limiting form for small arguments and the identities from the generalized function as shown below [15]

$$\lim_{r_{ij} \rightarrow 0} H_1^{(1)}(kr_{ij}) = kr_{ij} / 2 + 2i / (\pi kr_{ij}), \quad (20)$$

$$\lim_{r_{ij} \rightarrow 0} H_2^{(1)}(kr_{ij}) = (kr_{ij})^2 / 8 + 4i / (\pi (kr_{ij})^2). \quad (21)$$

The kernels in Eqs. (18) and (19) have the same singularity order as the Laplace equation. Therefore, Eqs. (14) and (15) for multiply-connected domain problems can be regularized by using the above mentioned regularization of subtracting and adding-back technique [12, 13] as follows:

$$\begin{aligned}
 u(x_i^I) &= \sum_{j=1}^{N_1} T(s_j^I, x_i^I) \alpha_j + \cdots + \sum_{j=N_1+\cdots+N_{p-1}+1}^{N_1+\cdots+N_p} T(s_j^I, x_i^I) \alpha_j \\
 &\quad + \cdots + \sum_{j=N_1+\cdots+N_{m-2}+1}^{N_1+\cdots+N_{m-1}} T(s_j^I, x_i^I) \alpha_j \\
 &\quad + \sum_{j=N_1+\cdots+N_{m-1}+1}^N T(s_j^O, x_i^I) \alpha_j \\
 &\quad - \sum_{j=N_1+\cdots+N_{p-1}+1}^{N_1+\cdots+N_p} \bar{T}(s_j^I, x_i^I) \alpha_i, \\
 x_i^I &\in B_p, \quad p = 1, 2, 3, \dots, m-1,
 \end{aligned} \quad (22)$$

where  $x_i^I$  is located on the inner boundary ( $p = 1, 2, 3, \dots, m-1$ ) and the superscripts  $I$  and  $O$  denote the inward and outward normal vectors, respectively, and

$$\begin{aligned}
 \sum_{j=N_1+\cdots+N_{p-1}+1}^{N_1+\cdots+N_p} \bar{T}(s_j^I, x_i^I) = 0, \quad x_i^I \in B_p, \\
 p = 1, 2, 3, \dots, m-1.
 \end{aligned} \quad (23)$$

Therefore, we can obtain

$$\begin{aligned}
 u(x_i^I) &= \sum_{j=1}^{N_1} T(s_j^I, x_i^I) \alpha_j + \cdots + \sum_{j=N_1+\cdots+N_{p-1}+1}^{i-1} T(s_j^I, x_i^I) \alpha_j \\
 &\quad + \sum_{j=i+1}^{N_1+\cdots+N_p} T(s_j^I, x_i^I) \alpha_j + \cdots \\
 &\quad + \sum_{j=N_1+\cdots+N_{m-2}+1}^{N_1+\cdots+N_{m-1}} T(s_j^I, x_i^I) \alpha_j \\
 &\quad + \sum_{j=N_1+\cdots+N_{m-1}+1}^N T(s_j^O, x_i^I) \alpha_j \\
 &\quad - \left[ \sum_{j=N_1+\cdots+N_{p-1}+1}^{N_1+\cdots+N_p} \bar{T}(s_j^I, x_i^I) - T(s_i^I, x_i^I) \right] \alpha_i, \\
 x_i^I &\in B_p, \quad p = 1, 2, 3, \dots, m-1.
 \end{aligned} \quad (24)$$

When the observation point  $x_i^O$  locates on the outer boundary ( $p=m$ ), Eq. (24) becomes

$$\begin{aligned}
 u(x_i^O) = & \sum_{j=1}^{N_1} T(s_j^I, x_i^O) \alpha_j + \sum_{j=N_1+1}^{N_1+N_2} T(s_j^I, x_i^O) \alpha_j + \dots \\
 & + \sum_{j=N_1+\dots+N_{m-1}}^{N_1+\dots+N_{m-1}} T(s_j^I, x_i^O) \alpha_j \\
 & + \sum_{j=N_1+\dots+N_{m-1}+1}^{i-1} T(s_j^O, x_i^O) \alpha_j \\
 & + \sum_{j=i+1}^N T(s_j^O, x_i^O) \alpha_j \\
 & - \left[ \sum_{j=N_1+\dots+N_{m-1}+1}^N \bar{T}(s_j^I, x_i^I) - T(s_i^O, x_i^O) \right] \alpha_i, \quad (25) \\
 & x_i^I \text{ and } O \in B_p, \quad p = m.
 \end{aligned}$$

Similarly, the boundary flux is obtained as

$$\begin{aligned}
 t(x_i^I) = & \sum_{j=1}^{N_1} M(s_j^I, x_i^I) \alpha_j + \dots + \sum_{j=N_1+\dots+N_{p-1}+1}^{i-1} M(s_j^I, x_i^I) \alpha_j \\
 & + \sum_{j=i+1}^{N_1+\dots+N_p} M(s_j^I, x_i^I) \alpha_j + \dots \\
 & + \sum_{j=N_1+\dots+N_{m-2}+1}^{N_1+\dots+N_{m-1}} M(s_j^I, x_i^I) \alpha_j \\
 & + \sum_{j=N_1+\dots+N_{m-1}+1}^N M(s_j^O, x_i^I) \alpha_j \\
 & - \left[ \sum_{j=N_1+\dots+N_{p-1}+1}^{N_1+\dots+N_p} \bar{M}(s_j^I, x_i^I) - M(s_i^I, x_i^I) \right] \alpha_i, \quad (26) \\
 & x_i^I \in B_p, \quad p = 1, 2, 3, \dots, m-1.
 \end{aligned}$$

$$\begin{aligned}
 t(x_i^O) = & \sum_{j=1}^{N_1} M(s_j^I, x_i^O) \alpha_j + \sum_{j=N_1+1}^{N_1+N_2} M(s_j^I, x_i^O) \alpha_j + \dots \\
 & + \sum_{j=N_1+\dots+N_{m-2}+1}^{N_1+\dots+N_{m-1}} M(s_j^I, x_i^O) \alpha_j \\
 & + \sum_{j=N_1+\dots+N_{m-1}+1}^{i-1} M(s_j^O, x_i^O) \alpha_j + \sum_{j=i+1}^N M(s_j^O, x_i^O) \alpha_j \quad (27) \\
 & - \left[ \sum_{j=N_1+\dots+N_{m-1}+1}^N \bar{M}(s_j^I, x_i^I) - M(s_i^O, x_i^O) \right] \alpha_i, \\
 & x_i^O \text{ and } I \in B_p, \quad p = m.
 \end{aligned}$$

The detailed derivations of Eq. (23) can be found in the reference [12]. According to the dependence of normal vectors for inner and outer boundaries [12], their relationships are

$$\begin{cases} \bar{T}(s_j^I, x_i^I) = -\bar{T}(s_j^O, x_i^O), & i \neq j \\ \bar{T}(s_j^I, x_i^I) = \bar{T}(s_j^O, x_i^O), & i = j \end{cases} \quad (28)$$

$$\begin{cases} \bar{M}(s_j^I, x_i^I) = \bar{M}(s_j^O, x_i^O), & i \neq j \\ \bar{M}(s_j^I, x_i^I) = \bar{M}(s_j^O, x_i^O), & i = j \end{cases} \quad (29)$$

where the left and right hand sides of the equal sign in Eqs. (28) and (29) denote the kernels for observation and source points with the inward and outward normal vectors, respectively.

## (2) Antiplane shear and antiplane piezoelectricity problems with multiple inclusions

When  $k$  approaches to zero, the above-mentioned formulation can be also applied to the Laplace problem with multiple holes, because of the same double-layer potentials for Helmholtz and Laplace problems.

### 2.4 Derivation of Influence Matrices

#### (1) Acoustic eigenproblem with a multiply-connected domain

By collocating  $N$  observation points to match with the BCs from Eqs. (24) and (25) for the Dirichlet problem, the linear algebraic equation is obtained

$$\begin{aligned}
 \begin{cases} \bar{u} \\ 0 \end{cases} = \begin{cases} \{0\} \\ [T] \end{cases} \begin{cases} \alpha \\ \alpha \end{cases} \Leftrightarrow \\
 \begin{cases} 0 \\ 0 \end{cases}_{N \times 1} = \begin{bmatrix} [T_{11}]_{N_1 \times N_1} & \dots & [T_{1m}]_{N_1 \times N_m} \\ \vdots & \ddots & \vdots \\ [T_{m1}]_{N_m \times N_1} & \dots & [T_{mm}]_{N_m \times N_m} \end{bmatrix}_{N \times N} \begin{cases} \alpha_1 \\ \vdots \\ \alpha_N \end{cases}_{N \times 1}, \quad (30)
 \end{aligned}$$

For the Neumann problem, Eqs. (26) and (27) yield

$$\begin{aligned}
 \begin{cases} \bar{t} \\ 0 \end{cases} = \begin{cases} \{0\} \\ [M] \end{cases} \begin{cases} \alpha \\ \alpha \end{cases} \Leftrightarrow \\
 \begin{cases} 0 \\ 0 \end{cases}_{N \times 1} = \begin{bmatrix} [M_{11}]_{N_1 \times N_1} & \dots & [M_{1m}]_{N_1 \times N_m} \\ \vdots & \ddots & \vdots \\ [M_{m1}]_{N_m \times N_1} & \dots & [M_{mm}]_{N_m \times N_m} \end{bmatrix}_{N \times N} \begin{cases} \alpha_1 \\ \vdots \\ \alpha_N \end{cases}_{N \times 1}, \quad (31)
 \end{aligned}$$

For the mixed-type problem, a linear combination of Eqs. (30) and (31) is required to satisfy the mixed-type BCs.

#### (2) Antiplane shear and antiplane piezoelectricity problems with multiple inclusions

The antiplane piezoelectricity problem with multiple inclusions is decomposed into two parts as shown in Fig. 3. One is the exterior problem for matrix with hole subjected to the far-displacement field and far-electric field, the other is the interior problem for each inclusion. The two boundary data of matrix and inclusion satisfy the interface conditions in Eqs. (10) and (11). Furthermore, the exterior problem for matrix with holes subjected to a far-displacement field and far-electric field can be superimposed by two systems as shown in Fig. 4. For an interior problem, the linear algebraic system can be obtained as:

$$\begin{cases} u_1 \\ \vdots \\ u_N \end{cases} = [T_q^I] \begin{cases} \alpha_1 \\ \vdots \\ \alpha_N \end{cases} = \begin{bmatrix} [T_{11}^I] & \dots & [T_{1N}^I] \\ \vdots & \ddots & \vdots \\ [T_{N1}^I] & \dots & [T_{NN}^I] \end{bmatrix} \begin{cases} \alpha_1 \\ \vdots \\ \alpha_N \end{cases}, \quad q \in w \text{ or } \phi, \quad (32)$$

$$\begin{cases} t_1 \\ \vdots \\ t_N \end{cases} = [M_q^I] \begin{cases} \alpha_1 \\ \vdots \\ \alpha_N \end{cases} = \begin{bmatrix} [M_{11}^I] & \dots & [M_{1N}^I] \\ \vdots & \ddots & \vdots \\ [M_{N1}^I] & \dots & [M_{NN}^I] \end{bmatrix} \begin{cases} \alpha_1 \\ \vdots \\ \alpha_N \end{cases}, \quad q \in w \text{ or } \phi, \quad (33)$$

where  $w$  and  $\phi$  denote the out-of-plane elastic displacement and in-of-plane electric potential, respectively.

For an exterior problem, we have

$$\begin{cases} u_1 \\ \vdots \\ u_N \end{cases} = [T_q^O] \begin{cases} \alpha_1 \\ \vdots \\ \alpha_N \end{cases} = \begin{bmatrix} [T_{11}^O] & \dots & [T_{1N}^O] \\ \vdots & \ddots & \vdots \\ [T_{N1}^O] & \dots & [T_{NN}^O] \end{bmatrix} \begin{cases} \alpha_1 \\ \vdots \\ \alpha_N \end{cases}, \quad q \in w \text{ or } \phi, \quad (34)$$

$$\begin{cases} t_1 \\ \vdots \\ t_N \end{cases} = [M_q^O] \begin{cases} \alpha_1 \\ \vdots \\ \alpha_N \end{cases} = \begin{bmatrix} [M_{11}^O] & \dots & [M_{1N}^O] \\ \vdots & \ddots & \vdots \\ [M_{N1}^O] & \dots & [M_{NN}^O] \end{bmatrix} \begin{cases} \alpha_1 \\ \vdots \\ \alpha_N \end{cases}, \quad q \in w \text{ or } \phi. \quad (35)$$

Substituting Eqs. (32), (33), (34) and (35) into Eqs. (10) and (11), the linear algebraic system for antiplane piezoelectricity problem is obtained as:

$$\begin{bmatrix} -[T_w^I] & [T_w^O] & 0 & 0 \\ 0 & 0 & -[T_\phi^I] & [T_\phi^O] \\ -\frac{c_{44}^i}{c_{44}^m}[M_w^I] & -[M_w^O] & -\frac{e_{15}^i}{c_{44}^m}[M_\phi^I] & -\frac{e_{15}^m}{c_{44}^m}[M_\phi^O] \\ -[M_w^I] & -\frac{e_{15}^m}{e_{15}^i}[M_w^O] & \frac{e_{11}^i}{e_{15}^i}[M_\phi^I] & \frac{e_{11}^m}{e_{15}^i}[M_\phi^O] \end{bmatrix} \begin{Bmatrix} \alpha_w^i \\ \alpha_w^m \\ \alpha_\phi^i \\ \alpha_\phi^m \end{Bmatrix} = \begin{Bmatrix} -\{w^\infty\} \\ -\{\phi^\infty\} \end{Bmatrix} + \frac{e_{15}^m}{c_{44}^m} \left\{ \frac{\partial \phi^\infty}{\partial n} \right\} + \frac{e_{15}^i}{e_{15}^m} \left\{ \frac{\partial w^\infty}{\partial n} \right\} - \frac{e_{11}^m}{e_{15}^i} \left\{ \frac{\partial \phi^\infty}{\partial n} \right\} \right)^T, \quad (36)$$

The unknown densities  $(\{\alpha_w^i\}, \{\alpha_w^m\}, \{\alpha_\phi^i\}, \{\alpha_\phi^m\})$  in Eq. (36) can be obtained by implementing the linear algebraic solver and the stress concentration can be solved by using Eq. (6).

For the antiplane shear problem with multiple inclusions, we obtain

$$\begin{bmatrix} -[T_w^I] & [T_w^O] \\ -\frac{\mu^i}{\mu^m}[M_w^I] & -[M_w^O] \end{bmatrix} \begin{Bmatrix} \alpha_w^i \\ \alpha_w^m \end{Bmatrix} = \begin{Bmatrix} -\{w^\infty\} \\ \left\{ \frac{\partial w^\infty}{\partial n} \right\} \end{Bmatrix}, \quad (37)$$

where  $\mu^i$  and  $\mu^m$  are equal to  $c_{44}^i$  and  $c_{44}^m$ , respectively.

## 2.5 Extraction of the Eigenvalues

### (1) Acoustic eigenproblem with a multiply-connected domain

In order to sort out the eigenvalues, the SVD technique is utilized [9]. We obtain Eqs. (30) and (31) by using the double-layer potentials approach for the Dirichlet and Neumann problems, respectively. Form Eqs. (30) and (31), we can obtain eigenvalues by using the SVD technique as follows:

$$[T] = [\Phi_T] [\Sigma_T] [\Psi_T]^H, \quad (38)$$

$$[M] = [\Phi_M] [\Sigma_M] [\Psi_M]^H, \quad (39)$$

where the superscript  $H$  denotes the transpose and conjugate,  $\Sigma_T$  and  $\Sigma_M$  are diagonal matrices with diagonal elements of positive or zero singular values and  $[\Phi_T]$ ,  $[\Phi_M]$ ,  $[\Psi_T]$  and  $[\Psi_M]$  are the left and right unitary matrices corresponding with  $[T]$  and  $[M]$ , respectively. Thus the minimum singular value of  $[T]$  or  $[M]$  as a function of  $k$  can be utilized to detect the eigenvalue and eigenmodes by using unitary vectors. However, spurious eigenvalues are present for a multiply-connected domain eigenproblem. Spurious eigenvalue can be extracted out by using SVD updating term techniques as shown in the next section.

## 2.6 Treatments of Spurious Eigenvalues

### (1) Acoustic eigenproblem with a multiply-connected domain

In order to sort out the spurious eigenvalues, the SVD updating term is utilized [9]. We can combine Eqs. (30) and (31) by using the SVD updating term as follows:

$$[P]\{\alpha\} = \begin{bmatrix} [T]_{N \times N} \\ [M]_{N \times N} \end{bmatrix} \{\alpha\} = \{0\}. \quad (40)$$

The rank of the matrix  $[P]$  must be smaller than  $2N$  to have a spurious mode [9]. By using the SVD technique, the matrix in Eq. (40) can be decomposed into

$$[P] = \begin{bmatrix} \Phi_T & 0 \\ 0 & \Phi_M \end{bmatrix} \begin{bmatrix} \Sigma_T & 0 \\ 0 & \Sigma_M \end{bmatrix} \begin{bmatrix} \Psi_T & 0 \\ 0 & \Psi_M \end{bmatrix}^H. \quad (41)$$

Based on the equivalence between the SVD technique and the least-squares method, we extract out the spurious eigenvalue by detecting zero singular values for  $[P]$  matrix.

## 3. Numerical examples

In order to show the accuracy and validity of the proposed method, four numerical examples are considered.

### Case 1 Antiplane shear problem

Fig. 5 shows the matrix imbedded three inclusions under antiplane shear. The geometry conditions is  $d = 2r_1$ . It is interesting to note that a uniform stress field results when the shear modulus is the same for the inclusion and the matrix. Therefore, the stress concentrations  $\sigma_{z\theta}$  in the matrix around the interface of the first inclusion are shown in Fig. 6 (a)~(d), respectively. From Fig. 6 (a), it is obvious that the case of holes ( $\mu_1/\mu_0 = \mu_2/\mu_0 = \mu_3/\mu_0 = 0.0$ ) leads to the maximum stress concentration at  $\theta = 0^\circ$ . Because of the interaction effects, it is larger than 2 of a single hole [6]. The stress component  $\sigma_{z\theta}$  vanishes in the case of approximation to rigid inclusions ( $\mu_1/\mu_0 = \mu_2/\mu_0 = \mu_3/\mu_0 = 5.0$ ). The results are compared with those of the Laurent series expansion method [7].

### Case 2 Antiplane piezoelectricity problem

The single piezoelectric inclusion in a piezoelectric matrix is shown in Fig. 7. In this case, the remote shear, shear modulus, piezoelectric modulus, dielectric modulus and elastic modulus are  $\tau = 5 \times 10^7 \text{ Nm}^{-2}$ ,  $e_{15}^i = 10.0 \text{ Cm}^{-2}$ ,  $e_{11}^m = e_{11}^i = 1.51 \times 10^{-8} \text{ CV}^{-1}\text{m}^{-1}$  and  $c_{44}^m = c_{44}^i = 3.53 \times 10^{10} \text{ Nm}^{-2}$ , respectively. Stress concentrations versus different piezoelectric modulus ratio are shown in Fig. 8 (a)~(b) for the case of  $E = -10^6 \text{ V/m}$ . When  $E = -10^6 \text{ V/m}$  and  $e_{15}^m/e_{15}^i = -10$  for the negative poling direction, the negative maximum stress concentration occurs in the matrix of  $\theta = 0$  as shown in Fig. 8 (a). However, the positive maximum stress concentration occurs in the matrix of  $\theta = \pi/2$  as shown in Fig. 8 (b). Good agreement is made after comparing with the analytical solution [3].

### Case 3 Acoustic eigenproblem

The inner and outer radii of domain are  $r_1 = 0.5$  and  $r_2 = 2.0$ , respectively. All the boundary conditions are the Dirichlet type ( $u = 0$ ) and Neumann type ( $t = 0$ ) as shown in Fig. 9. The analytical solutions of true eigenequations [9] for Dirichlet and Neumann types, respectively, are shown below:

$$J_n(kr_1)Y_n(kr_2) - J_n(kr_2)Y_n(kr_1) = 0, \text{ (Dirichlet)} \quad (42)$$

$$J_n'(kr_1)Y_n'(kr_2) - J_n'(kr_2)Y_n'(kr_1) = 0, \text{ (Neumann)}. \quad (43)$$

The analytical solutions of spurious eigenequations [9] for both types are the same as:

$$J_n'(kr_1) = 0. \quad (44)$$

The minimum singular value versus wave number by using our proposed method for the Dirichlet and Neumann BCs are shown in Fig. 10(a) and (b),

respectively. Good agreement is obtained after comparing with analytical solutions. The spurious eigenvalues for the Dirichlet and Neumann problems are found out by employing SVD updating term as shown in Fig. 10(c). From Fig. 10(c), we find that one spurious eigenvalue appear at  $k_s = 3.68 (J_1^1)$  in the range of  $0 < k \leq 5$ . This spurious eigenvalue is found to be the true eigenvalue of Neumann eigenproblem of an interior circular domain with a radius 0.5.

#### Case 4 Acoustic eigenproblem with four equal holes

In this case, the eigenvalues were obtained by Chen and his coworkers [16]. The radius  $R$  of outer boundary is 1.0 and the eccentricity  $e$  and radius  $c$  of the inner circular boundaries are 0.5 and 0.1, respectively. Dirichlet problem is considered as shown in Fig. 11. The former five eigenvalues by using the RMM, BEM, FEM and PM are listed in Table 1, where the results of PM miss the eigenvalues of  $k_2$  and  $k_3$ . In this case, no spurious eigenvalue is found in the range of  $0 < k < 6$  since the first spurious eigenvalue is 18.412 ( $J_1^1$ ). The eigenvalues of  $k_2$  and  $k_3$  are roots of multiplicity two by finding the second successive zero singular value in SVD when using RMM and BEM. Besides, the symmetry of the fourth mode shape by using the PM is quite different from the results of RMM and BEM. The former five eigenmodes of the RMM and the BEM are shown in Fig. 12. Agreeable results of the RMM are obtained by comparing with the BEM data.

## 4. CONCLUSION

In this study, we employed the RMM to solve three engineering problems. Only the boundary nodes on the physical boundary are required. The major difficulty of the coincidence of the source and collocation points in the conventional MFS is then circumvented. Furthermore, the controversy of the fictitious boundary outside the physical domain by using the conventional MFS no longer exists. Although it results in the singularity and hypersingularity due to the use of double-layer potential, the finite values of the diagonal terms for the influence matrices have been determined by employing the regularization technique. The numerical results were obtained by applying the developed program to solve antiplane shear and antiplane piezoelectricity problems and acoustic eigenproblems through four examples. Numerical results agreed very well with the analytical solution and those of BEM, FEM and PM.

## 5. ACKNOWLEDGEMENT

Financial support from the National Science Council under Grant No. NSC-95-2221-E-464-003-MY3 to the second author for Toko University is gratefully acknowledged.

## 6. REFERENCES

- [1] J.L. Bleustein, "New surface wave in piezoelectric materials," *Appl. Phys. Lett.*, vol. 13, pp. 412-413, 1968.
- [2] Y.E. Pak, "Circular inclusion problem in antiplane piezoelectricity," *Int. J. Solids Struct.*, vol. 29, pp. 2403-2419, 1992.
- [3] T. Honein, B.V. Honein, "On the interaction of two piezoelectric fibers embedded in an intelligent material," *J. Intell. Mater. Syst. Struct.*, vol. 6, pp. 229-236, 1995.
- [4] T. Chen, S.C. Chiang, "Electroelastic fields and effective moduli of a medium containing cavities or rigid inclusions of arbitrary shape under anti-plane mechanical and in-plane electric fields," *Acta Mech.*, vol. 121, pp. 79-96, 1997.
- [5] C.K. Chao, K.J. Chang, "Interacting circular inclusion in antiplane piezoelectricity," *Int. J. Solids Struct.*, vol. 36, pp. 3349-3373, 1999.
- [6] E. Honein, T. Honein, G. Herrmann, "On two circular inclusions in harmonic problems," *Q. Appl. Math.*, vol. 50, pp. 479-499, 1992.
- [7] S.X. Gong, "Antiplane interaction among multiple circular inclusions," *Mech. Res. Commun.*, vol. 22, pp. 257-262, 1995.
- [8] J.T. Chen, J.H. Lin, S.R. Kuo, S.W. Chyuan "Boundary element analysis for the Helmholtz eigenvalue problems with a multiply connected domain", *Proc. Roy. Soc. Lond., Ser. A*, vol. 457, pp. 2521-2546, 2001.
- [9] J.T. Chen, L.W. Liu, H.K. Hong, "Spurious and true eigensolutions of Helmholtz BIEs and BEMs for a multiply connected problem", *Proc. Roy. Soc. Lond., Ser. A*, vol. 459, pp. 1891-1924, 2003.
- [10] J.T. Chen, M.H. Chang, K.H. Chen, S.R. Lin "The boundary collocation method with meshless concept for acoustic eigenanalysis of two-dimensional cavities using radial basis function", *J. Sound Vib.*, vol. 257, pp. 667-711, 2002.
- [11] V.D. Kupradze, M.A. Aleksidze, "The method of functional equations for the approximate solution of certain boundary value problems," *USSR Comput. Math. Math. Phys.*, vol. 4, pp. 199-205, 1964.
- [12] D.L. Young, K.H. Chen, C.W. Lee, "Novel meshless method for solving the potential problems with arbitrary domain," *J. Comput. Phys.*, vol. 209, pp. 290-321, 2005.
- [13] K.H. Chen, J.H. Kao, J.T. Chen, D.L. Young, M.C. Lu, "Regularized meshless method for multiply-connected-domain Laplace problems," *Eng. Anal. Bound. Elem.*, vol. 30, pp.882-896, 2006.
- [14] D.L. Young, K.H. Chen, C.W. Lee, "Singular meshless method using double layer potentials for exterior acoustics," *J. Acoust. Soc. Am.*, vol. 119, pp. 96-107, 2005.
- [15] M. Abramowitz, I.A. Stegun, "Handbook of mathematical functions with formulation graphs and mathematical tables," *New York. Dover.*, 1972.
- [16] J.T. Chen, L.W. Liu, S.W. Chyuan, "Acoustic eigenanalysis for multiply-connected problems using dual BEM," *Commun. Numer. Methods Engng.*, vol. 20, pp. 419-440, 2004.

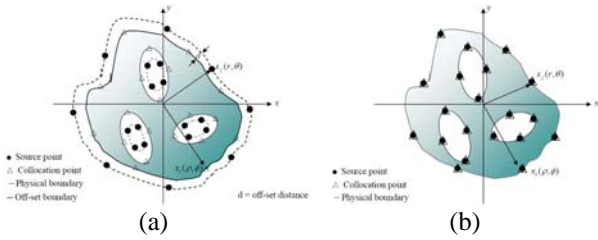


Fig. 1 The distribution of the source points and observation points and definitions of  $r, \theta, \rho, \phi$  by using the (a) conventional MFS, (b) RMM.

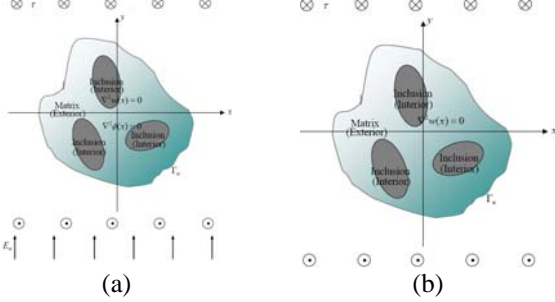


Fig. 2 Problem sketch for (a) antiplane piezoelectricity and (b) antiplane shear problems with multiple inclusions.

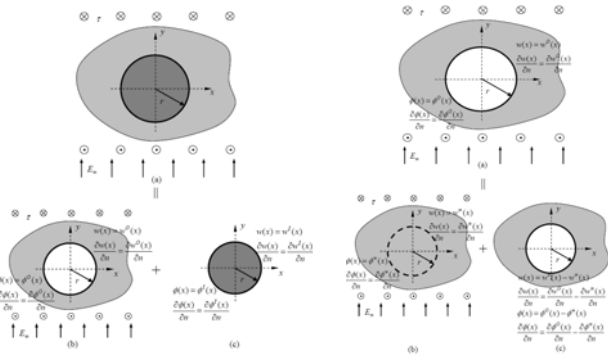


Fig. 3 Decomposition of the problem.

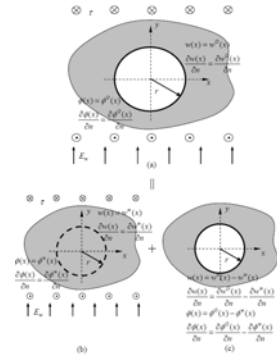


Fig. 4 Decomposition of the problem of Fig. 3(b).

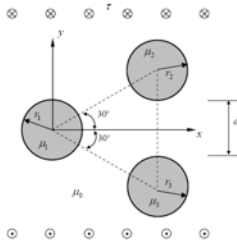


Fig. 5 Problem sketch of three inclusions under antiplane shear.

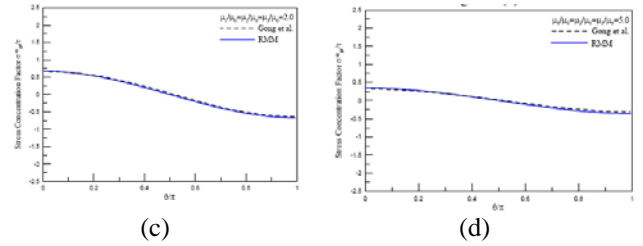
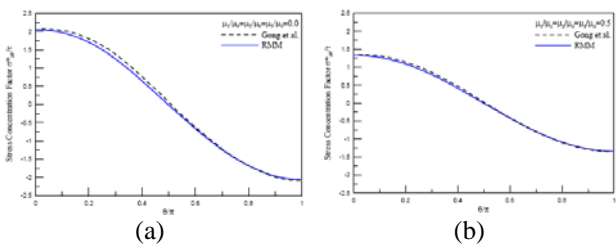


Fig. 6 Stress concentration factor  $\sigma_{z0}^m/\tau$  along the boundaries of both the left inclusion and matrix for various different shear modulus ratios.

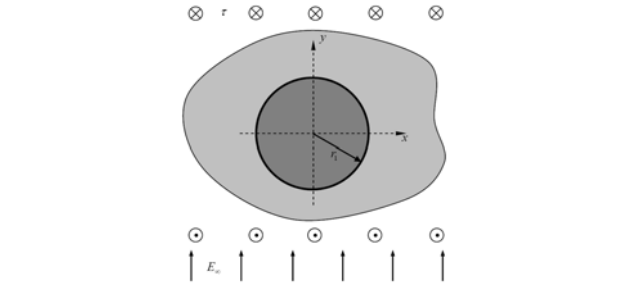


Fig. 7 Problem sketch of a single piezoelectric inclusion.

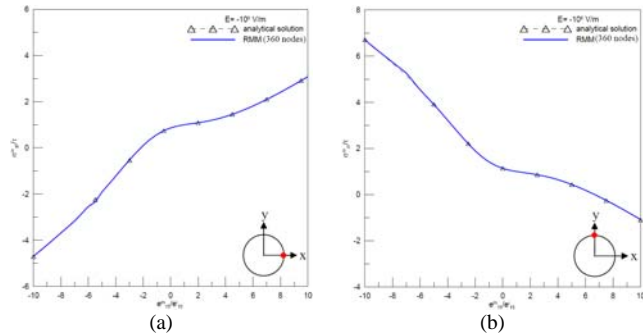


Fig. 8 Stress concentration result of single piezoelectric inclusion in piezoelectric matrix for different piezoelectric modulus ratios when  $E = -10^6$  V/m, (a)  $\theta = 0$ , (b)  $\theta = \pi/2$

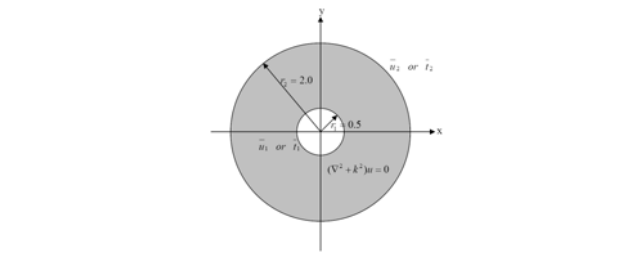


Fig. 9 Problem sketch for an annular eigenproblem.

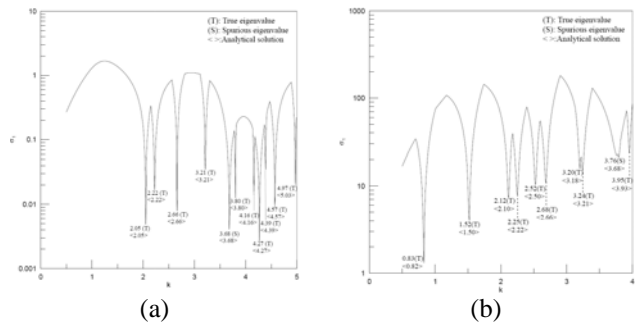


Fig. 10 True eigenvalue, Spurious eigenvalue, and Analytical solution.

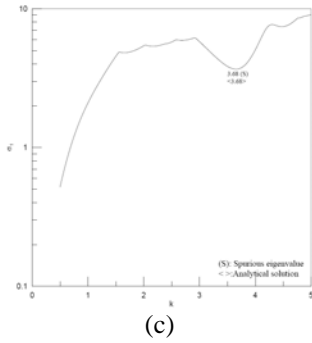


Fig. 10 The result of RMM and analytical solution for the (a) Dirichlet BC, (b) Neumann BC, (c) SVD updating term.

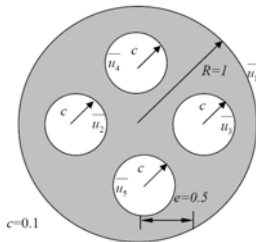


Fig. 11 Problem sketch for an acoustic eigenproblem with four equal holes.

Eigenvalue \ Method	RMM	BEM	FEM	PM
$k_1$	4.50(SS)	4.47(SS)	4.443	4.655(SS)
$k_2$	5.38(AS)	5.37(AS)	5.316	N/A
$k_3$	5.38(SA)	5.37(SA)	5.320	N/A
$k_4$	5.55(AA)	5.54(AA)	5.486	5.561(SA)
$k_5$	5.95(SS)	5.95(SS)	5.884	5.868(SS)

Table 1 The former five eigenvalues for a circular domain with four equal holes by using different approaches.

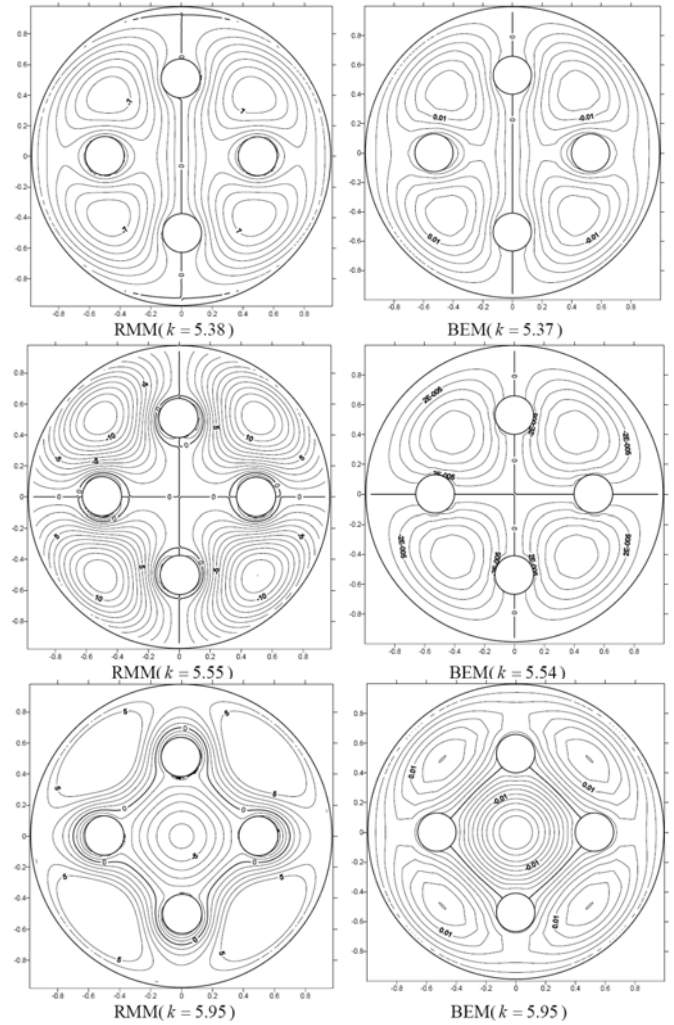
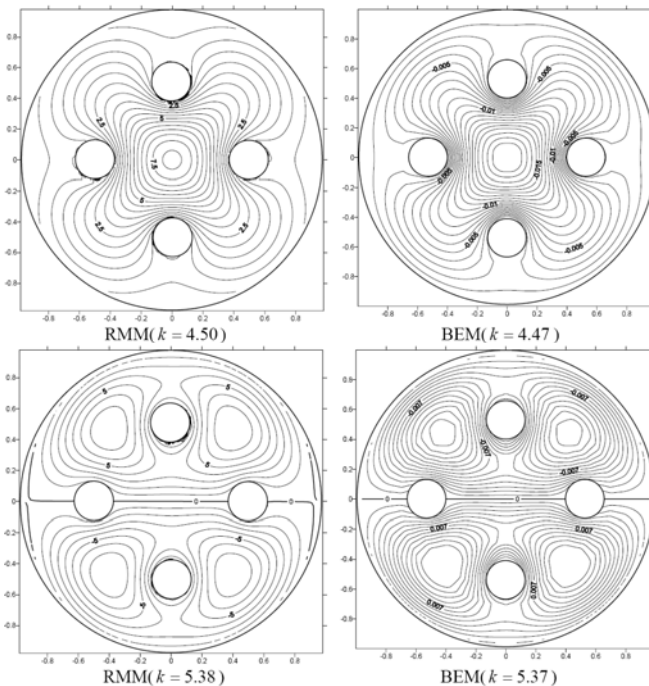


Fig. 12 Eigenmodes of the RMM and BEM for the case 4.



## 正規化無網格法在工程上之應用

高政宏<sup>1</sup> 陳桂鴻<sup>2</sup> 陳正宗<sup>1</sup>

1 國立台灣海洋大學河海工程系  
 2 稻江科技暨管理學院資訊管理系

### 摘要

本文藉由正規化無網格法求解含多夾雜之反平面剪力及反平面壓電材問題與多連通聲場特徵值問題。以雙層勢能來表示整個場解，並配合一加一減技巧來正規化處理奇異及超奇異核函數。我們所提出的方法有別於傳統基本解法須將源點佈在虛假邊界上，可將奇異源放在真實的邊界上。最後，數值結果將與解析解，邊界元素法，有限元素法及配點法做比較，獲得一致性的結果。

**關鍵詞：**正規化無網格法，一加一減法，基本解法，壓電，多夾雜，多孔洞，假根，聲場。